JOURNAL OF SCIENCE
SAKARYA UNIVERSITY

Sakarya University Journal of Science

ISSN 1301-4048 | e-ISSN 2147-835X | Period Bimonthly | Founded: 1997 | Publisher Sakarya University | http://www.saujs.sakarya.edu.tr/en/

Title: Investigation of Beam Width Shaping of a Ku-band Horn Antenna using a Diffractive Optic Element and an Electromagnetic Wave Absorber

Authors: Ahmet TEBER
Recieved: 2020-04-25 21:21:40

Accepted: 2020-06-17 14:10:33

Article Type: Research Article
Volume: 24
Issue: 5
Month: October
Year: 2020
Pages: 819-831

How to cite
Ahmet TEBER; (2020), Investigation of Beam Width Shaping of a Ku-band Horn Antenna using a Diffractive Optic Element and an Electromagnetic Wave Absorber. Sakarya University Journal of Science, 24(5), 819-831, DOI: https://doi.org/10.16984/saufenbilder.726905
Access link
http://www.saujs.sakarya.edu.tr/en/pub/issue/56422/726905

Sakarya University Journal of Science 24(5), 819-831, 2020

Investigation of Beam Width Shaping of a Ku-band Horn Antenna using a Diffractive Optic Element and an Electromagnetic Wave Absorber

Ahmet TEBER [*1]

Abstract

The feasibility of beam-shaping of a Ku-Band horn as a transmitting (Tx) antenna by mounting two different versions of lenses which are kind of Fresnel Zone Plates (FZP) is studied. The designed and fabricated geometrical structures offer a simpler approach building Fresnel Zone Plates by using an electromagnetic wave absorber and diffractive optic material. The diffractive optic material, paraffin, forms a set of alternating open and opaque annular zones on a flat surface, based on the design principles of Fresnel Zone Plates. An electromagnetic wave absorber covers the top surface of the formed paraffin, but not including the grooves. Thereafter, the Fresnel Zone plates are suitably attached in front of the transmitter horn antenna, located in the far-field region of a receiving antenna. The half-power beam-widths for the horn antenna (unloaded) and with two types of lenses are investigated. The results indicate that Fresnel zone plate structures can play a role suppressing side lobes in H-plane so that the effective radiation is to be significantly concentrated.

Keywords: Beam-width, diffractive optic elements, electromagnetic wave absorber, Fresnel zone plates, horn antenna

1. INTRODUCTION

A Fresnel antenna incorporates a set of concentric annular zones called Fresnel zones [1-3]. Depending on the geometry and the fabrication material of Fresnel Zones, the Fresnel antenna can be classified as the Fresnel lens or Fresnel Zone Plates (FZPs). Unless the lens is very thin, a theoretical analysis of the Fresnel structure can complicate. Therefore, FZPs have been taking place of the Fresnel lenses in recent years [4-8]. The applications of FZPs in millimeter/centimeter wave regions were uncommon in the past, because of their relatively low gain, controlling by shaping side/back lobes, in comparison with that of parabolic reflector antennas [2]. With advances in active devices, it is no longer a problem to increase the transmitted power and engineers have

* Corresponding Author: ahmetteber@bayburt.edu.tr
[1] Bayburt University, Department of Electricty and Energy, Bayburt, Turkey.
ORCID: https://orcid.org/0000-0002-7361-2302

been implementing different types of FZPs to deal with it.

Diffractive optic elements can be used for focusing (including focusing into an arbitrary area), filtration, polarization and formation, splitting and mixing of radiation beams in the GHz region [9-12]. In this work, paraffin wax is used as a diffractive optic material with low weight, high diffraction efficiency, high spatial resolution dictated by the diffraction limit, simple fabrication technology, and the feasibility of manufacturing FZPs on arbitrary surfaces. Other than that, Teflon which has a similar permittivity with paraffin, can be another diffractive optic material. But, it requires molding with a lathe workbench. Therefore, it is not preferred by us for this study. The other important part of the FZPs is electromagnetic wave absorbers (EMWAs), which have been used in various aerospace and defense applications [13-16]. In this study, manganese soft spinel ferrites blended with multi-walled carbon nanotubes as an EMWA were molded as toroid-shaped pellets with 1 mm thickness, suitable for the Ku-Band horn antenna aperture. The crystal structure, morphology, and magnetic nature of composites as well as the microwave absorption properties of the EMWA have been discussed in detail in our published works [14, 16]. The circular FZPs fit within the rectangular aperture of the antenna. According to the model of FZPs, either the odd-numbered zones or the even-numbered zones are covered with the absorbing material. When the even-numbered zones are covered with an absorbing material, there exists 180 degree phase correction. Odd-numbered zones are covered by the absorbing material in this study.

The horn antenna is utilized particularly at microwaves frequencies, yet straightforward antenna for many applications such as communication satellite antennas and radio telescopes etc. since they have no resonant elements. For a particular application of horn antenna, for example a ground-penetrating radar (GPR), antennas must achieve high gain, narrow beam, low side lobe and reflection characteristics over the wide band to attain the powerful and adequately shaped radiation [17]. In antenna technologies, many claims about directivity of radar antennas, direction-finding equipment, indoor applications are for improving their side lobe performances [18]. The radiation patterns with the scenario of a far-field region on the horn antenna (unloaded) and the horn antenna with the absorbing material and diffractive optic element at the frequency of Ku-band are obtained. It was observed that there exists a reduction in both main lobe and side lobe levels due to the usage of absorber layer. This reduction was distributed as a portion in between the main lobe and side/rear lobes, causing the beam-width of antenna to be shaped. Another point that draws attention in this study is to attract attention to the fact that the beam-width of the antenna can be shaped with the help of absorber material. Therefore, the study suggests that absorbing material as thin layer can play a role on beamforming whereas controlling main and side/back lobes in Ku-band. In E-plane, the main lobe of the horn antenna loaded with the absorbing layer and a diffractive optic element is decreased whereas side lobes are increased when there are no significant changes on rear lobes at all frequencies that is measured. According to the angles of two orthogonal planes, the elevation angles of a horn antenna with the absorbing layer are obtained less than the transmitter (Tx) horn antenna (unloaded) in H-plane that means the suppressed side and back lobes are obtained. It has apparently lower side-lobes compared with the horn antenna (unloaded) in the H-plane, demonstrating that an absorbing material can effectively be used to reduction of side lobes and concentrating the main lobe in the forward direction. Moreover, beam-width shaping is quite important to enhance horn antenna gain for these applications. For that purpose, we claim that absorbing materials in the field of antennas can be used in a design of lens that is relatively new to concentrate the desired radiation without reducing distortion and bending with narrower beam width. Traditionally, using curved bends are used to avoid reflections by then antenna. In some of studies on beamforming antenna applications, the inside of antenna can be re-fabricated that causes sharp bends. It often results in increase reflections and mode distortions inherently reduce the transmitted power through the bend. In our design we did not make any changes of antenna structure,

which is one of the advantage of our work. In that way the losses by distortion and bending is prevented. In this experimental study, Fresnel Zone Plates serve how affects beam-shaping of a standard gain horn antenna. We investigated that the feasibility of two designs of Fresnel Zone Plates on beamforming in the GHz frequency range. For this purpose, first, an electromagnetic wave absorber was used from our previous work and the FZP Models were designed (using the design rules of the FZPs with absorbing / transparent zones) and fabricated.

Radiation pattern measurements obtained transmission parameters (S_{21}) were carried out and significant antenna parameter, namely Half-Power Beam-Widths (HPBWs), were determined to understand how the HPBWs change. In order to plot radiation patterns in E- and H-plane S_{21} transfer parameters are used, which are obtained by vector network analyzer. All the measurements are done using quasi-anechoic chamber that we set up using pyramidal microwave absorbers. In that way, the reflections nearby objects which distort the radiation patterns are minimized. As known, S_{21} represents the power transferred from transmitter antenna to receiving antenna. It is also known that S_{21} is zero implies that all power delivered to receiving antenna. According to S21 measurement results, the radiation patterns in E-plane and H-plane are plotted with that aspect.

2. DESIGN OF FRESNEL ZONE PLATES

2.1. Design Procedure of Zone Plates

Fresnel zones composed of a set of concentric strips are arranged on a flat surface. The strips alternate between absorbing and transmitting layers. The geometrical configurations in Figure 1 are used throughout this work.

The FZP zones are annular for the considered normal incidence. The operating principle of the FZP has been described in detail at [1] and [17]. The FZP radiation characteristics are given by the more precise physical optics current method in [18].

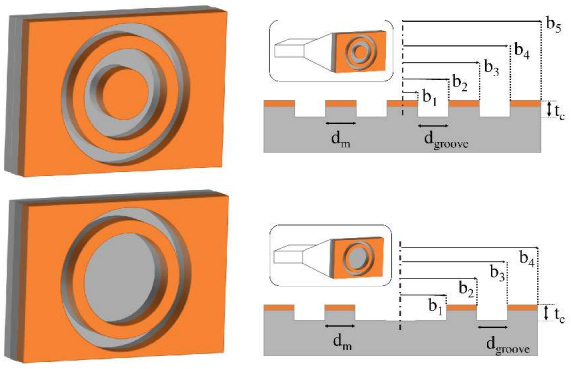

Figure 1 The design of Fresnel Zone Plates (a) Type 1 as shown on the top-left, (b) The side view of Type 1 as shown on the top-right, (c) Type 2 as shown on the bottom-left, (d) The side view of Type 2 as shown on the bottom-right

The transmission mode of FZP concentrates energy from the incident wave on one side to focus on the other side. The focusing effect is produced by the diffraction or the second radiation on the open and opaque ring surfaces. Depending on the material these zones are made of, we have two lens types of FZPs: lenses with absorbing/transparent (a/t) zones and lenses with phase-correcting (p/c) zones. Those lenses are designed below by using the Fresnel zone plate theory. The radii of the FZP rings are determined with the n-th radii, bn, given by [1]:

$$b_n = \sqrt{\frac{2n\lambda}{P}\left(F + \frac{n\lambda}{2P}\right)} \qquad (1)$$

where F, the focal length of the zone plates, equals to zero in this study and λ is the wavelength. According to the distances from a selected focal point, the consecutive radii of these zones are chosen on the central axis increase by a value of λ while going from the inner to the outer radius of any zone.

There exists a lower boundary limit for the difference between two consecutive radii: $dgroove = \lambda/P$ in Ref 1. P equals to two for the FZPA absorbing/transparent (a/t) zones, which means that if a plane wave is normally incident to the zone plate, the portions of the radiation, which pass through the various transparent zones, all reach by diffraction the focal point $z = -F$ with mutual phases that differ less than 180 degrees.

When a/t-zones are used, the odd-numbered zones are covered with absorbing material. We did not consider that the influence on the radiation pattern of Fresnel zones of which the width of zones $d_m = (b_{n+1} - b_n)/2$ is in the order of a few wavelength or even smaller in [1]. Therefore, dm is constant value in this work. Reference [1] shows that not only the number of zones decreases with F but also d_m decreases with the radius of b_n. Nevertheless, the absorbing material with wider radii to keep them on the same dB level covers the last zone compatible with the dimensions on the horn antenna. The radius of zone plates for n values are listed in Table 1.

Table 1
The radius of the zones

n	2n	b_n	dgroove	d_m
1	2	0.83	0.83	0.415
2	4	1.66	0.83	0.415
3	6	2.49	0.83	0.415
4	8	3.32	0.83	0.415
5	10	4.29	0.97	0.415

The radius of zones for n values of selected absorbing/transparent zones by using focal length (F) equals to zero and P equals to two and λ, wavelength is 1.66 cm. According to the geometrical configuration of the Fresnel antenna [1], focal distance is assumed zero since the FZP lens in this study is mounted to the feed (transmitter (Tx) horn antenna) without any gap. Thus, the successive radius are calculated using the Equation 1 whereas F is zero as a lower limit for the differences between successive radii λ/P (F=0). The values of design parameters are calculated by using Equation 1. The depth of a groove can now be derived by calculating the phase delay of the wave in the dielectric or the paraffin as diffraction optic material with respect to the wave in free space. Then the following relation must be valid:

$$(k_x - k)t_c = \pi, \;\; k_x = k\sqrt{\varepsilon_r} \qquad (2)$$

the wave number (k) in the diffraction optic material, and the relative dielectric constant of the material ε_r, the latter equation can be written as

$$k(\sqrt{\varepsilon_r} - 1)t_c = \pi \qquad (3)$$

The groove depth, t_c is defined by [12]:

$$t_c = \frac{\lambda_0}{2\sqrt{\varepsilon_r} - 1} \qquad (4)$$

where ε_r=2.5 (the paraffin wax relative permittivity for paraffin wax) and the groove depth is 0.83 cm.

In this study, there are two type of zone plates as Type-1 and Type-2. The only difference in between them is absence of the section covered with the absorbing material at the center of the layer in Type-2. The zone radii are the same for Type-1 and -2 except the absence of center zone in Type-1.

2.2. Preparation of Electromagnetic Wave Absorbers (EMWAs)

The EMWA resulting from manganese soft spinel ferrite nano-particles (MF NPs) with multi-walled carbon nanotubes were prepared by a citric acid assisted sol-gel method whereas MWCNTs were purchased from US Research Nanomaterials, Inc., USA. The crystal structure, morphology, magnetic property and microwave absorption behavior were discussed in detail [13, 14]. According to the ring sizes mentioned above, the absorber rings are created with 1 mm thickness using the fabrication technique in [16]. The diffraction optic material of paraffin and the absorber with a toroidal-shape are attached to each other using epoxy glue with a very small thickness. Finally, the structures are mounted to the horn antenna in Figure 1.

3. EXPERİMENTAL SETUP OF RADİATİON PATTERNS

The radiation pattern is a graphical representation of the strength of radiation of a horn antenna as a function of direction. The given antenna is located at the origin of a spherical polar coordinates system (r, θ, φ) and the variation in the field strength at different points on an imaginary concentric spherical surface of radius r is noted. For a sufficiently larger r, the radiation pattern is independent or r and the fields are tangential to the hypothetical spherical surface. In general, separate patterns are plotted for θ and φ

polarization [18-20]. The experimental setup of radiation pattern measurements is demonstrated in Figure 2. All directivity measurements were carried out in the laboratory environment with the experimental setup that is covered by pyramidal absorbers to reduce reflections from the walls, except on top of the measurement platform. The transmitting and the receiving antennas are set them up at an appropriate distance (approximately 2 meter) above the surface of the wooden table. A receiving antenna is considered to be from transmitter antenna with the material under test (MUT) in the far-field region. The distance with the transmitter and the receiving antennas is formulated on the condition of far-field region. r is the value of the distance a transmitting antenna from the receiving antenna, D (3.32 cm x 4.29 cm of inside dimensions of the horn antenna of WR62-15 dB) is the largest dimension of the receiver and transmitter horn antenna [20] and λ cm is the wavelength.

3.1. Measurement Procedure of E- and H-Plane Radiation Patterns

The antennas were positioned for the maximum meter reading and this position of the receiving antenna is marked as 0 degree. We kept the distance between the antennas constant and sufficiently large according to the distance (r) with the transmitter and the receiving antennas. We continually rotated the receiving horn clockwise, in steps of 2 degrees, to cover 360 degrees including the main, side and back lobes. At each position, we took care keeping the initial setup of the calibrated vector network analyzer (VNA) to restore the 2 degrees' scale deflection. We returned to the position 0 degree and repeated for the other plane in steps of 2-degree scale deflection on clockwise until completion of the 180 degree. Then we took into account the symmetry of all acquired data, which is field strength versus angle, so that the entire radiation pattern were obtained for E-plane on x-z plane as shown on Figure 2. The same procedure with E-Plane was repeated for y-z plane to obtain data of H-plane pattern. We finally plotted the radiation pattern in the above manner for both E- and H-planes after acquiring the data for H-Plane.

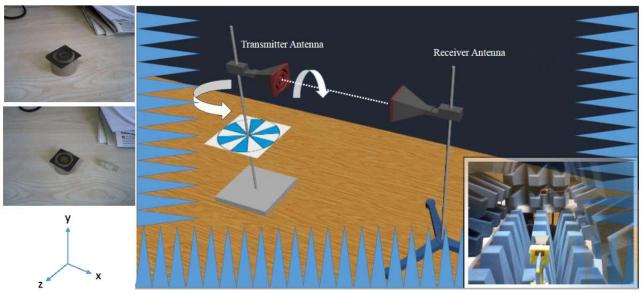

Figure 2 Fabricated Fresnel zone plates and the experimental setup: radiation field of a horn antenna with the Fresnel Zone Plates

4. RESULTS AND DISCUSSION

We have performed an experimental study of the beam-width forming with the scenario of a far-field radiation patterns on horn antenna (unloaded), a horn antenna with Types 1 and 2 at the seven frequencies (12.4, 13, 14,…,18 GHz) when the FZPs are attached to the transmitter antenna. Here, the azimuth and elevation half-power beam-width angles obtained are listed in Table 2.

Table 2
E- and H- Plane beam-widths

f (GHz)	**E-PLANE (degree)**			**H-PLANE (degree)**		
	Air Horn	Type 1	Type 2	Air Horn	Type 1	Type 2
12.4	30.48	18.94	65.08	33.74	25.20	28.80
13	30.48	13.18	33.36	31.92	17.50	23.26
14	27.58	17.50	47.78	30.48	15.68	22.64
15	20.38	11.74	34.80	30.18	17.40	21.32
16	23.26	14.62	34.80	29.86	15.52	19.62
17	23.26	17.50	36.66	25.16	13.46	18.08
18	22.82	16.24	43.66	19.82	13.72	15.74

We observed that the narrowest beam-width (BW) in both E- and H- Planes was obtained for a standard gain horn antenna with Type 1 of FZP. Depending on the beam-widths values, the narrower (smaller than the horn antenna with Type 1 of FZP) beam-widths in E-Plane was obtained for a standard gain horn antenna (unloaded) and horn antenna with Type 2 of FZP, respectively. In H-Plane, the beam-width of the horn antenna (unloaded) is larger than the beam-width of the horn antenna with Type 2 FZP. In addition, we found that the side lobe levels were

suppressed in H-Plane and the side-lobes in the E-Plane were higher than the side-lobes in the H-Plane. It has apparently lower side-lobes compared with the horn antenna (unloaded), demonstrating that one can effectively reduce side-lobes of the horn antenna by attaching the FZPs. According to the results, the horn antenna with Type 1 FZP shows that a good performance in the Ku-band whereas an absorbing material caused an effect on the side lobes because of that the absorbing materials on the zones are not infinitely thin, which caused a shadowing effect [21]. Note that FZP reduces the quadratic phase error at horn's aperture plane, however, the radiation efficiency, reflection loss and cross-pol performance due to FZP must be considered. In this study we have performed an experimental study using empirical data resulting from the measurement of transmission parameter S_{21}.

4.1. E-Plane Radiation Patterns (in Polar Coordinates) of Horn Antenna (unloaded), Horn Antenna with Type 1 and 2

The experimental far-field radiation patterns (E-Plane) of the scenario with the real structures of FZPs at seven sample frequencies (12.4 through 18 GHz) are shown in Figure 3. It is observed that the beam-widths of horn antenna with Type-1 at each frequency in E-plane have the smallest values. The beam-width values of horn antenna with Type-2 in E-plane are obtained higher than the beam-width values of horn antenna with Type-1 and smaller than the beam-width values of horn antenna (unloaded), respectively. Note that all directivity measurements are done in the scale of dB.

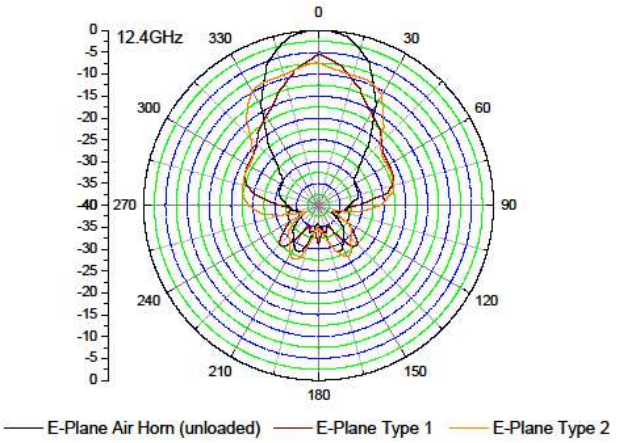

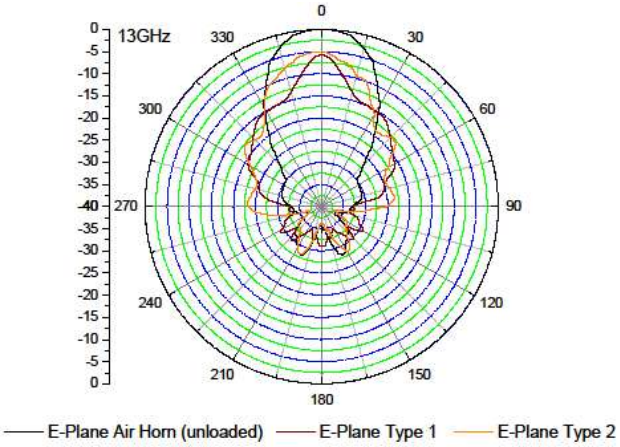

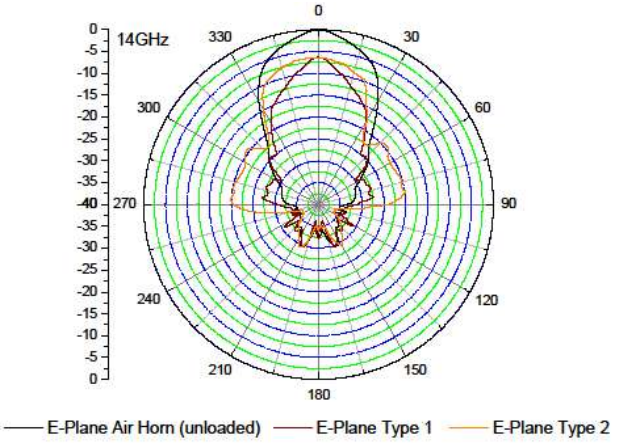

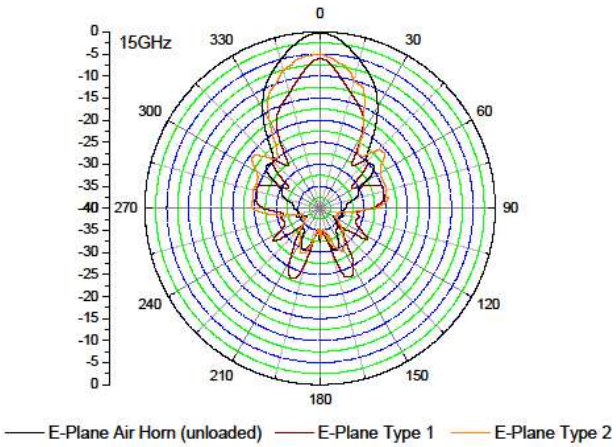

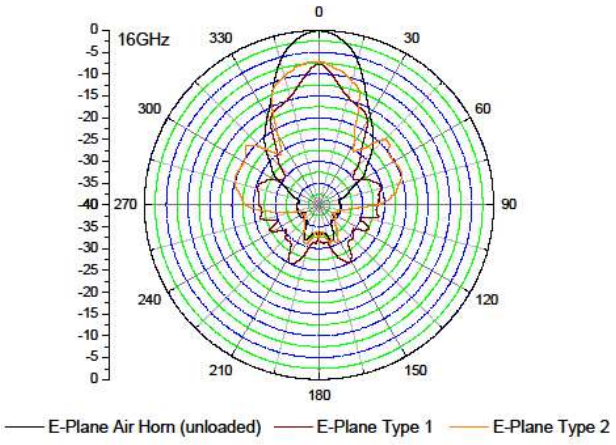

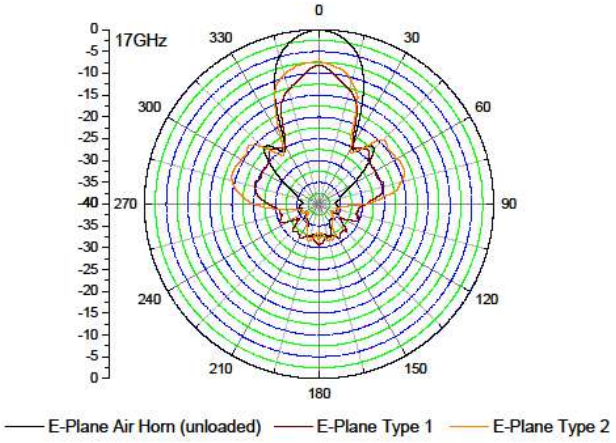

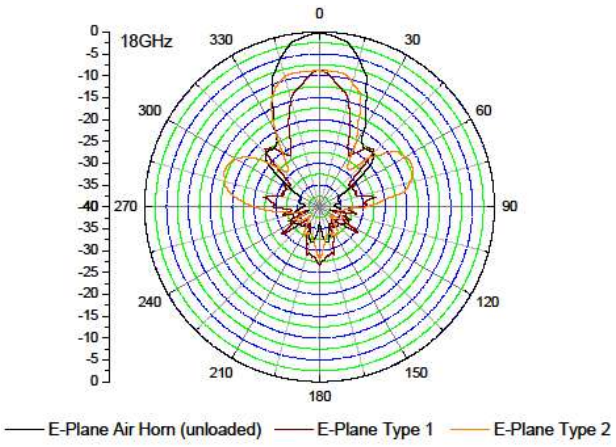

Figure 3 The comparison of the radiation patterns in E-Plane (12.4 GHz through 18 GHz) including the transmitter horn antenna (unloaded), the transmitter antenna with type 1 (wine color), and the transmitter antenna with type 2 (orange color) FZP

4.2. H-Plane Radiation Patterns (in Polar Coordinates) of Horn Antenna (unloaded), Horn Antenna with Type 1 and 2

The experimental far-field radiation patterns (H-Plane) of the scenario with the real structures of FZPs at seven sample frequencies (12.4 through 18 GHz) are shown in Figure 4. It is observed that the beam-widths of horn antenna with Type-1 at each frequency in H-plane have the smallest values. The beam-width values of horn antenna with Type-2 in H-plane are obtained higher than the beam-width values of horn antenna with Type-1 and smaller than the beam-width values of horn antenna (unloaded), respectively.

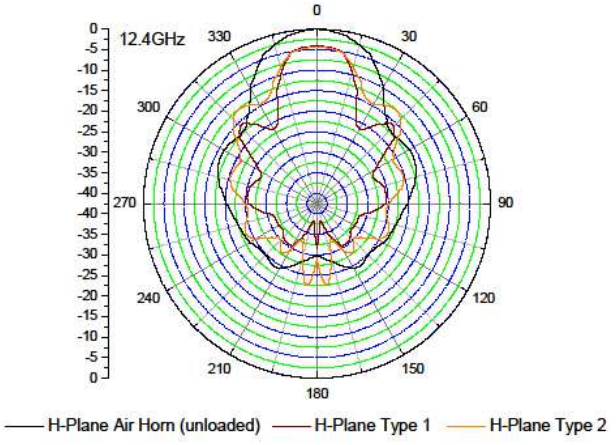

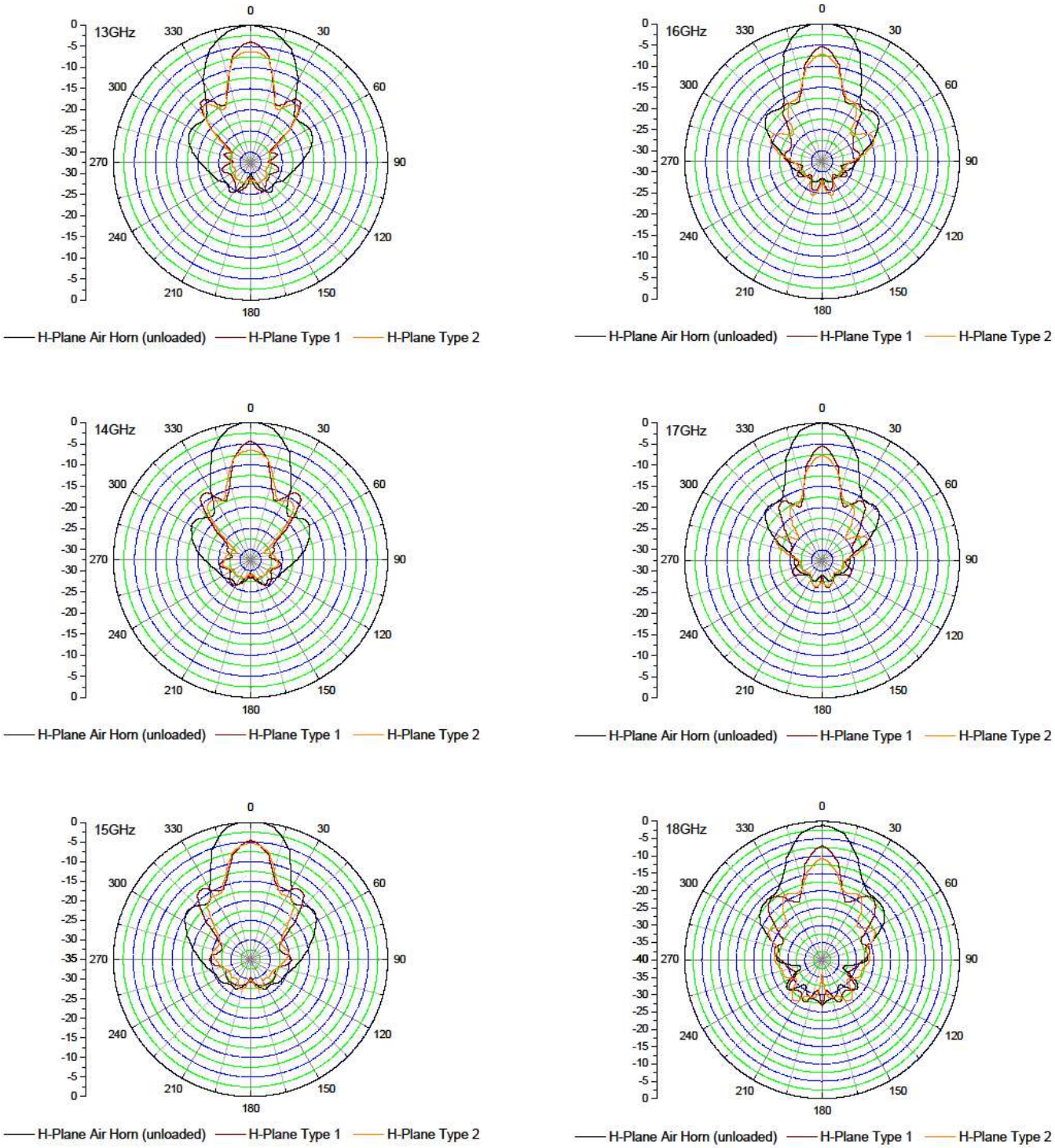

Figure 4 The comparison of the radiation patterns in H-Plane (12.4 GHz through 18 GHz) including the transmitter horn antenna (unloaded), the transmitter antenna with Type 1 (wine color), and the transmitter antenna with Type 2 (orange color) FZP

In E-plane, the main lobe of the horn antenna loaded with the absorbing layer and diffractive optic element is decreased whereas side lobes are increased when there are no significant changes on rear lobes at all frequencies that is measured. According to the angles of two orthogonal planes, the elevation angles of a horn antenna with the absorbing layer are obtained less than the transmitter (Tx) horn antenna (unloaded) in H-plane that means the suppressed side and back lobes are obtained. Horn antenna with Type-1 and Type-2 has apparently lower side-lobes compared with the horn antenna (unloaded) in the H-plane.

4.3. Measured Radiation Patterns (Diagonal Plane) in the E-Plane of Horn Antenna (unloaded), Horn Antenna with Type 1 and 2

The experimental far-field radiation patterns (E- and H-Plane) in diagonal plane are shown in Figure 5 and Figure 6.

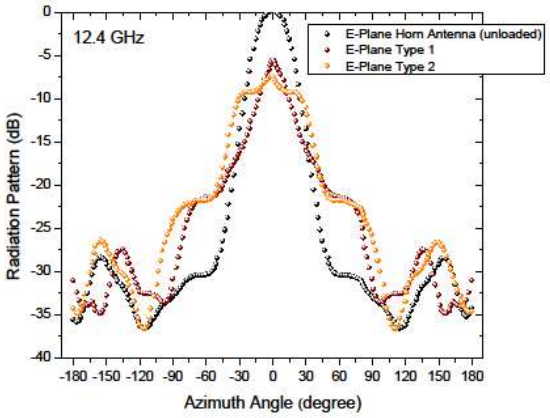

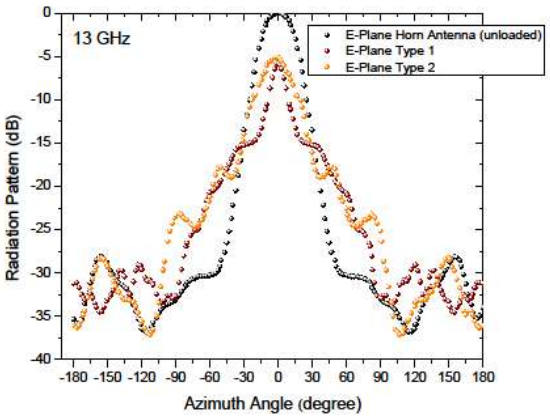

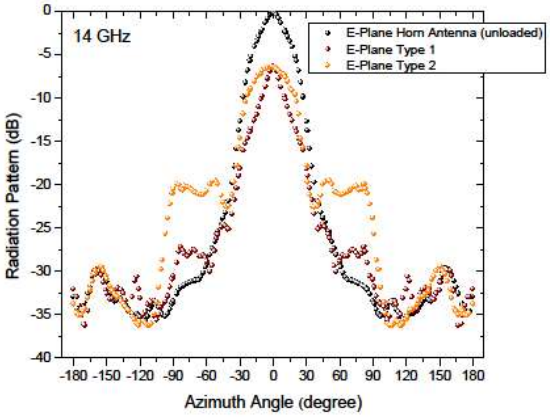

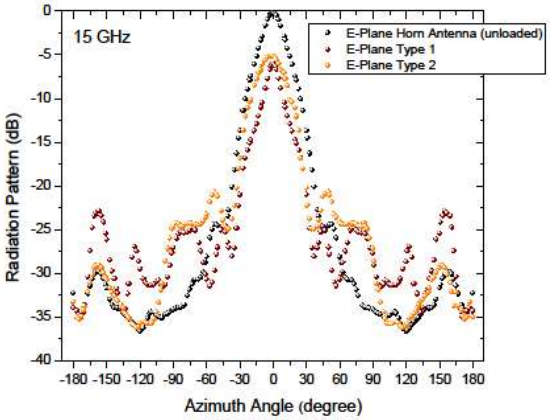

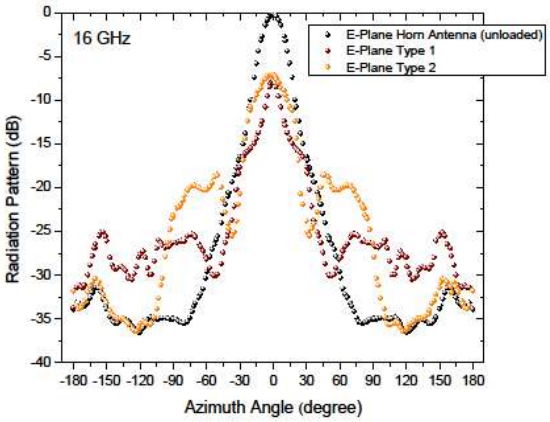

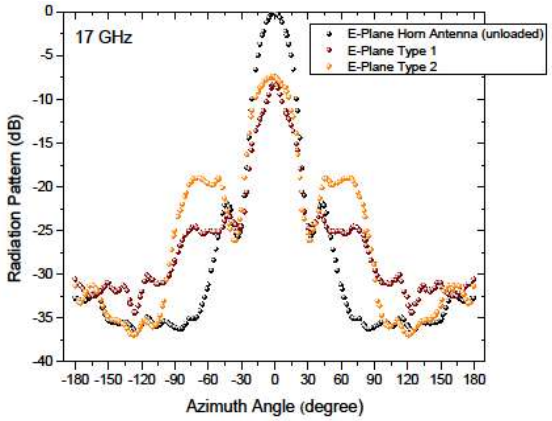

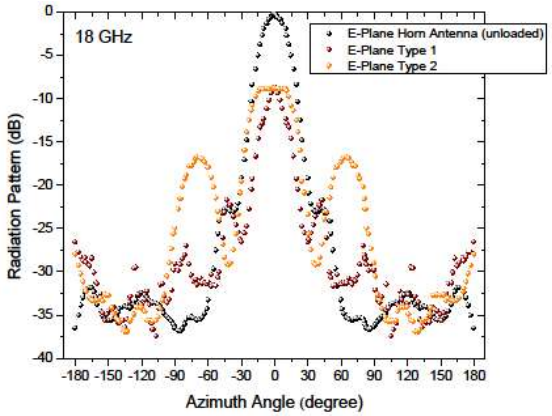

Figure 5 Measured far-field radiation patterns in E-Plane (12.4 GHz through 18 GHz) including the transmitter horn antenna (unloaded), the transmitter antenna with Type 1 (wine color), and the transmitter antenna with Type 2 (orange color) FZP

4.4. Measured Radiation Patterns (Diagonal Plane) in the H-Plane of Horn Antenna (unloaded), Horn Antenna with Type 1 and 2

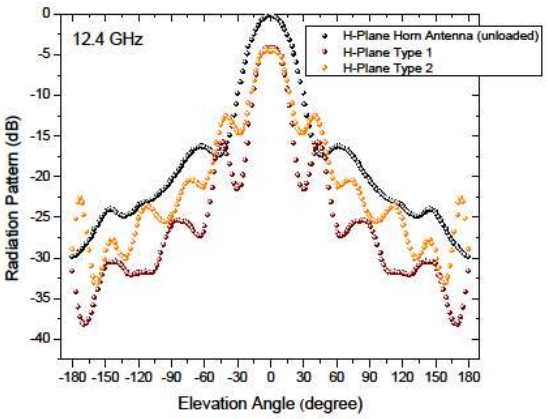

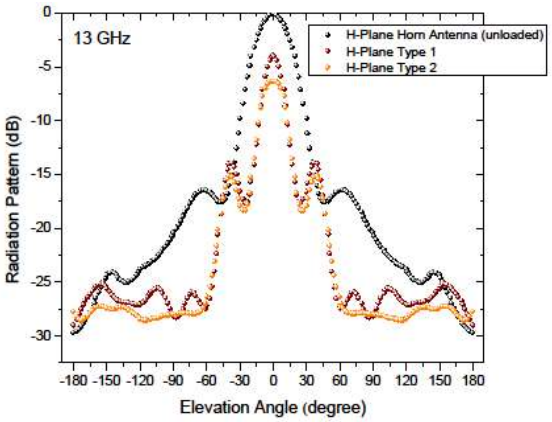

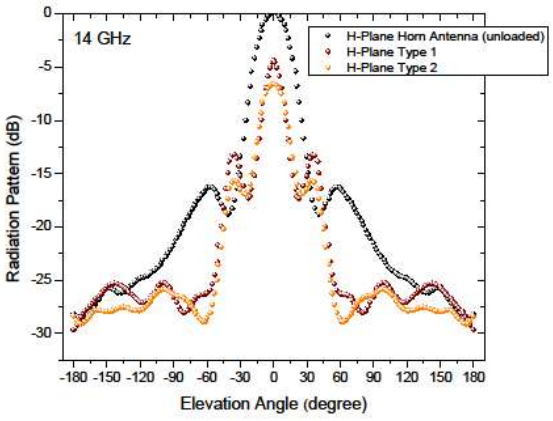

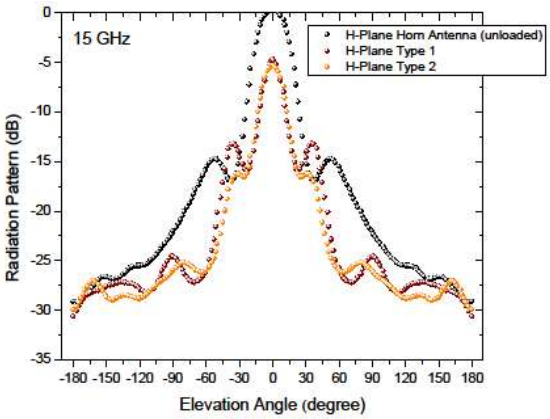

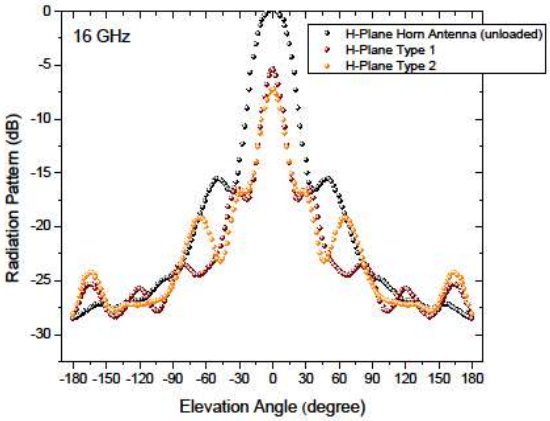

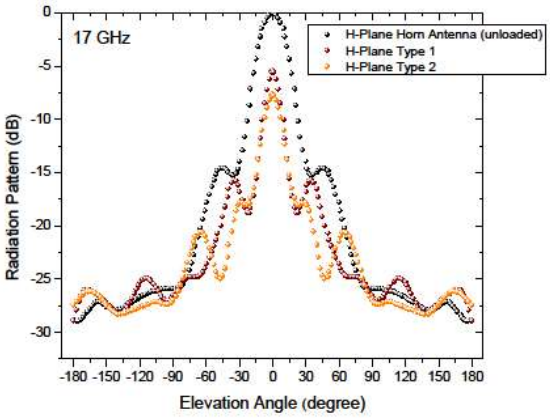

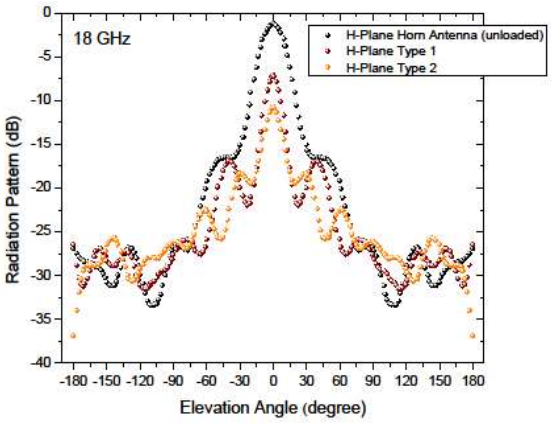

Figure 6 Measured far-field radiation patterns in H-Plane (12.4 GHz through 18 GHz) including the transmitter horn antenna (unloaded), the transmitter antenna with Type 1 (wine color), and the transmitter antenna with Type 2 (orange color) FZP

5. CONCLUSION

We have presented beamforming of the transmitting horn antenna by using two types of Fresnel Zone Plates in the Ku-band. We observed how paraffin as a diffractive optic material and the manganese soft spinel ferrites with multi-walled carbon nanotubes as an electromagnetic wave absorber that affect the radiation patterns, demonstrating that an absorbing material can effectively be used to reduction of side/back lobes and main lobe. Beyond that, an absorber material and a diffractive optic material can be a good solutions, concentrating the main lobe in the forward direction at many applications depending on their features. The results show that with Type 1 FZP provides narrower beam-widths in E- and H- Plane whereas the side lobe levels are suppressed in H-plane. Therefore, this study offers that electromagnetic wave absorbers as a thin layer structure and diffractive optic element of paraffin can play a role on beamforming that is controlled by side and back lobes. As it is known, the approximate antenna gain depends on the angle values at the points where the beam widths in E- and H- planes are reduced by 3dB. However, one of the Kraus and Tai & Pereira equations should be used in the antenna gain calculation depending on the 39.77 degree which is a critical value for these angle values. If the beam angles

are less than 39.77 degrees, antenna gain can be calculated using the Kraus and Tai & Pereira equations. It is obviously seen that suppressing side/back lobes are associate with the antenna gain. Therefore, it will be possible to increase the antenna gain in relation to suppress the beam widths of the side lobes and the rear lobe. By taking into consideration the relationship between beam width and antenna gain. This article has unique advantages to tune antenna gain. In this respect, this article is thought to make a significant contribution to the literature in terms of antenna gain increase. Therefore. This article will lead future studies on antenna gain, taking into account beam width results.

Funding

The author received no financial support for the research, authorship, and/or publication of this paper.

The Declaration of Conflict of Interest/ Common Interest

No conflict of interest or common interest has been declared by the author.

The Declaration of Ethics Committee Approval

The author declares that this document does not require an ethics committee approval or any special permission.

The Declaration of Research and Publication Ethics

The author of the paper declares that he complies with the scientific, ethical and quotation rules of SAUJS in all processes of the paper and that he does not make any falsification on the data collected. In addition, he declares that Sakarya University Journal of Science and its editorial board have no responsibility for any ethical violations that may be encountered, and that this study has not been evaluated in any academic publication environment other than Sakarya University Journal of Science.

REFERENCES

[1] L. C. J. Baggen, "The Fresnel Zone Plate Antenna: design and analysis", Eindhoven Univ. of Tech., Eindhoven, Netherlands, 1992.

[2] G. I. Greisukh, E. G. Ezhov, A. V. Kalashnikov, I.A. Levin and S.A. Stepanov, "The efficiency of relief-phase diffractive elements at a small number of Fresnel zones," Optics and Spectroscopy, vol. 113, no. 4, pp. 425-430, 2012.

[3] J. C. Wiltse, "Recent developments in Fresnel zone plate antennas at microwave/millimeter-wave," In Optical Devices and Methods for Microwave/Millimeter-wave and Frontier Applications, vol. 3464, pp. 146-154, 1998.

[4] H. D. Hristov, "Fresnel Zones in Wireless Links, Zone Plate Lenses and Antennas," Artech House, Inc., 2000.

[5] J. Pourahmadazar, S. Sahebghalam, S.A. Aghdam, M.A. Nouri, "Millimeter-wave Fresnel zone plate lens design using perforated 3D printing material," In 2018 IEEE MTT-S International Microwave Workshop Series on Advanced Materials and Processes for RF and THz Applications (IMWS-AMP), pp. 1-3, 2018.

[6] S. M. Stout-Grandy, A. Petosa, I. V. Minin, O. V. Minin, J. S. Wight, "Novel reflector-backed Fresnel zone plate antenna," Microwave and Optical Technology Letters, vol. 49, no. 12, pp. 3096-3098, 2007.

[7] A. Jouade, J. Bor, M. Himdi, O. Lafond, "Millimeter-wave Fresnel zone plate lens with new technological process," International Journal of Microwave and Wireless Technologies, vol. 9, no. 4, pp. 939-944, 2017.

[8] X. Liu, Y. Y. Chen, Y. Ge, "Wideband High-Efficiency Fresnel Zone Plate Reflector Antennas Using Compact

Subwavelength Dual-Dipole Unit Cells," Progress in Electromagnetics Research, vol. 86, pp. 29-39, 2018.

[9] L. C. J. Baggen, M. H. A. J. Herben, "Design procedure for a Fresnel-zone plate antenna," Int. J. Infrared and Millimeter Waves, vol. 14, no. 6, pp. 1341-1352, 1993.

[10] J. C. Wiltse, "Millimeter-wave Fresnel zone plate antenna," Millimeter and Microwave Engineering for Communications and Radar: A Critical Review, International Society for Optics and Photonics, vol. 10276, pp. 1027605, 1994.

[11] I. Minin and O. Minin, "Diffractive optics and nanophotonics: Resolution below the diffraction limit," Switzerland, Springer, 2015.

[12] S. T. Bobrov, G. I. Greisukh and Y. G. Turkevich, "Design procedure for a Fresnel-zone plate antenna," Mashinostroenie, pp. 223, 1986.

[13] A. Teber, R. Bansal, I. S. Unver and Z. Mehmedi, "The measurement of microwave absorption characteristics of nanocomposites using a coaxial line technique," Int. J. High Speed Electronics and Systems, vol. 27, no. 01n02, pp. 1840011, 2019.

[14] A. Teber, K. Cil, T. Yilmaz, B. Eraslan, D. Uysal, G. Surucu, A. Baykal and R. Bansal, "Manganese and zinc spinel ferrites blended with multi-walled carbon nanotubes as microwave absorbing materials," Aerospace, vol. 4, no. 1, pp. 2, 2017.

[15] A. Teber, I.S. Unver, H. Kavas, B. Aktas and R. Bansal, "Knitted radar absorbing materials (RAM) based on nickel–cobalt magnetic materials," Journal of Magnetism and Magnetic Materials, vol. 406, pp. 228-232, 2016.

[16] A. Teber, "Development of radar absorbing materials (RAMs) based on nano-structured magnetic materials and applications," Dept. Elect. Eng., Univ. of Connecticut, Storrs, Connecticut, Doctoral Dissertation, pp. 1532, 2017.

[17] A. Mahmoudi and R. Afzalzadeh, "Analysis, design and fabrication of centimeter-wave dielectric Fresnel zone plate lens and reflector," The European Physical Journal-Applied Physics, vol. 32, no. 2, 2005.

[18] E. Pettinelli, P. M. Barone, E. Mattei, A. Di Matteo, F. Soldovieri, A. S. Turk, A. K. Hocaoglu and A. A. Vertiy, "Archaeology and cultural heritage," Subsurface Sensing, pp. 644-667, 2011.

[19] R. E. Collins, "Antennas and radiowave propagation," New York: McGraw-Hill, 1985.

[20] C. Balanis, "Antenna theory analysis and design," New Jersey: John Wiley & Sons. Inc., 2005.

[21] D. N. Black and J. C. Wiltse, "Millimeterwave characteristics of phase-correcting Fresnel zone plates," IEEE Transactions on Microwave Theory and Techniques, vol. 35, no. 12, pp. 1122-1129, 1987.